JOC Article
pubs.acs.org/joc

Ion−Molecule Reactions of *O*,*S*-Dimethyl Methylphosphonothioate: Evidence for Intramolecular Sulfur Oxidation during VX Perhydrolysis

Andrew M. McAnoy,*[,†] Jillianne Williams,[†] Martin R. L. Paine,[‡] Michael L. Rogers,[†] and Stephen J. Blanksby*[,‡]

[†]*Human Protection and Performance Division, Defence Science and Technology Organisation, 506 Lorimer St., Fishermans Bend, Victoria 3207, Australia, and* [‡]*School of Chemistry, University of Wollongong, Wollongong, New South Wales 2522, Australia*

andrew.mcanoy@dsto.defence.gov.au; blanksby@uow.edu.au

Received September 8, 2009

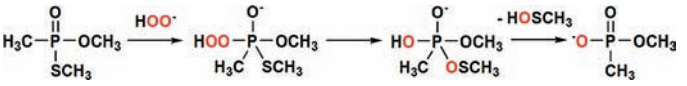

The alkaline perhydrolysis of the nerve agent *O*-ethyl *S*-[2-(diisopropylamino)ethyl] methylphosphonothioate (VX) was investigated by studying the ion−molecule reactions of HOO^- with *O*,*S*-dimethyl methylphosphonothioate in a modified linear ion-trap mass spectrometer. In addition to simple proton transfer, two other abundant product ions are observed at *m*/*z* 125 and 109 corresponding to the *S*-methyl methylphosphonothioate and methyl methylphosphonate anions, respectively. The structure of these product ions is demonstrated by a combination of collision-induced dissociation and isotope-labeling experiments that also provide evidence for their formation by nucleophilic reaction pathways, namely, (i) S_N2 at carbon to yield the *S*-methyl methylphosphonothioate anion and (ii) nucleophilic addition at phosphorus affording a reactive pentavalent intermediate that readily undergoes internal sulfur oxidation and concomitant elimination of CH_3SOH to yield the methyl methylphosphonate anion. Consistent with previous solution phase observations of VX perhydrolysis, the toxic P−O cleavage product is not observed in this VX model system and theoretical calculations identify P−O cleavage to be energetically uncompetitive. Conversely, intramolecular sulfur oxidation is calculated to be extremely exothermic and kinetically accessible explaining its competitiveness with the facile gas phase proton transfer process. Elimination of a sulfur moiety deactivates the nerve agent VX and thus the intramolecular sulfur oxidation process reported here is also able to explain the selective perhydrolysis of the nerve agent to relatively nontoxic products.

Introduction

Over recent years, the threat of a nerve agent release in a civilian environment by a terrorist group, such as the 1995 nerve agent attack in a Tokyo subway system,[1] has provided the impetus for the enhancement of methods for nerve agent detection and decontamination.[2−5] The chemistry of nerve agent degradation by alkaline hydrolysis is well established; *O*-isopropyl methylphosphonofluoridate (GB) and *O*-pinacolyl methylphosphonofluoridate (GD) are known to degrade to their corresponding phosphonic acids within minutes while, conversely, the alkaline hydrolysis of *O*-ethyl *S*-[2-(diisopropylamino)ethyl] methylphosphonothioate (VX) occurs slowly.[6] In addition, alkaline hydrolysis of VX results in two products formed via thiolate elimination, to form relatively nontoxic ethyl methylphosphonic acid (EMPA), or ethoxide elimination, to form the highly toxic and persistent *S*-[2-(diisopropylamino)ethyl] methylphosphonthioic acid (EA 2192) (Scheme 1).

(1) Suzuki, T.; Morita, H.; Ono, K.; Maekawa, K.; Nagai, R.; Yazaki, Y.; Nozaki, H.; Aikawa, N.; Shinozawa, Y.; Hori, S.; Fujishima, S.; Takuma, K.; Sagoh, M. *Lancet* **1995**, *345*, 980–981.
(2) Eubanks, L. M.; Dickerson, T. J.; Janda, K. D. *Chem. Soc. Rev.* **2007**, *36*, 458–470.
(3) Giordano, B. C.; Collins, G. E. *Curr. Org. Chem.* **2007**, *11*, 255–265.
(4) Talmage, S. S.; Watson, A. P.; Hauschild, V.; Munro, N. B.; King, J. *Curr. Org. Chem.* **2007**, *11*, 285–298.
(5) Yang, Y. C.; Baker, J. A.; Ward, J. R. *Chem. Rev.* **1992**, *92*, 1729–1743.
(6) Yang, Y. C.; Berg, F. J.; Szafraniec, L. L.; Beaudry, W. T.; Bunton, C. A.; Kumar, A. *J. Chem. Soc., Perkin Trans. 2* **1997**, 607–613.

DOI: 10.1021/jo901944p Published on Web 11/17/2009

SCHEME 1. Products of VX Hydrolysis and Perhydrolysis

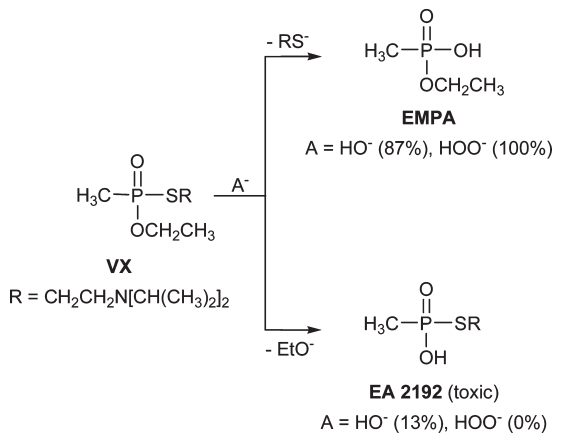

Peroxide-based decontaminants have also long been known to effectively degrade nerve agents[6−8] and an effective, environmentally benign decontaminant consisting of hydrogen peroxide and a peroxide activator in solution has been reported.[9] Interestingly, hydrogen peroxide alone in solution degrades GB very slowly with a half-life measured in the order of days, while the degradation of GB with an activated hydrogen peroxide solution occurs too rapidly to measure by NMR.[9] An additional benefit is that the perhydrolysis of VX also occurs rapidly under alkaline conditions and exclusively yields the nontoxic EMPA product.[6−8]

The disparity in product distribution between hydrolysis and perhydrolysis of VX is not fully understood. Addition−elimination processes at phosphorus are well-known to proceed via a pentavalent intermediate with nucleophilic attack and elimination preferentially occurring from the apical positions.[10,11] In addition, the more electronegative group prefers to be apical and so, in the absence of competing rearrangement processes, P−O cleavage may be expected to be favored over P−S cleavage as observed during the hydrolysis of cyclic phosphorothioates.[12] Conversely, the thiolate moiety is the more stable leaving group compared to the alkoxide group and should favor P−S over P−O cleavage. Pseudorotation between pentavalent intermediates, with an equilibrium favoring the thiol eliminating species, provides an explanation for the hydrolysis product distribution. However, it is difficult to account for the complete absence of P−O cleavage observed during VX perhydrolysis based on preferential pseudorotation alone. On the basis of their early experimental work, Yang et al. explained the preference for P−S cleavage by intramolecular oxygen transfer to sulfur, via a cyclic sulfonium ion, to yield a labile mixed anhydride that is readily hydrolyzed.[7] However, later work by Yang et al. on the alkaline perhydrolysis of *O*,*S*-diethyl methylphosphonothioate in $H_2{}^{18}O$ found no evidence for isotopic label incorporation into any reaction products and led to the proposition of an S_N2(phosphorus) mechanism for VX perhydrolysis with product selectivity due to relative basicities of the anionic nucleophile and leaving anions.[6] More recently, a theoretical study compared the alkaline hydrolysis and perhydrolysis of a VX model system and determined that both processes involve addition−elimination and proceed via respective phosphorus-centered pentavalent intermediates.[13] However, while reactions resulting in the direct cleavage of P−O and P−S bonds of the intermediates were calculated to be kinetically competitive during hydrolysis, only P−S bond cleavage was calculated to be kinetically favored during alkaline perhydrolysis and may explain the absence of the toxic product.[13]

Wagner et al. previously obtained ^{31}P NMR evidence for the elusive peroxyphosphonate intermediate in support of the GB and GD perhydrolysis mechanism in alkaline solution.[9] However, an analogous peroxy intermediate during VX perhydrolysis was not observed by ^{31}P NMR indicative of either a rapid reaction consuming the peroxy intermediate or an alternative mechanism for VX perhydrolysis. Interestingly, an alternative mechanism involving intramolecular sulfur oxidation within the pentavalent intermediate, with concomitant loss of the oxidized sulfur moiety, cannot be ruled out based on previous experimental data. Theoretical investigations into the perhydrolysis of VX and a model system indicate that the incipient hydroperoxide can transfer its nucleophilic oxygen to sulfur with the remaining hydroxide retained by the phosphorus atom.[13,14] These studies subdue concerns raised by the absence of ^{18}O incorporation during labeling studies that led to the proposal of an S_N2(phosphorus) mechanism.[6] Here we investigate the reactions of the putative perhydrolysis reagent HOO^- with *O*,*S*-dimethyl methylphosphonothioate (**1**), a VX model compound, to provide insight into the mechanism for the alkaline perhydrolysis of VX. In particular, our aims are to determine the effect of the methylthiolate on the gas phase reactivity at phosphorus as compared to analogous reactivity observed for dimethyl methylphosphonate (DMMP)[15] and to search for evidence, or otherwise, for the internal sulfur oxidation of the pentavalent intermediate.

Results and Discussion

In the absence of solvent effects, gas phase reactions of the hydroperoxide ion may provide insight into the efficacy and selectivity of nerve agent degradation by alkaline perhydrolysis. For example, the gas phase reactions of HOO^- with neutral DMMP are reported to undergo either an S_N2(carbon) process (89%) or proton transfer (11%).[15] These results contrast the trend where proton transfer dominates all other reported analogous reactions of anions of similar basicity to HOO^- ($\Delta_{acid}H_{300}$[HOOH] = 376.5 ± 0.4 kcal mol^{-1})[16] demonstrating the intrinsic nucleophilicity of the HOO^-

(7) Yang, Y. C.; Szafraniec, L. L.; Beaudry, W. T.; Bunton, C. A. *J. Org. Chem.* **1993**, *58*, 6964–6965.
(8) Yang, Y. C.; Szafraniec, L. L.; Beaudry, W. T.; Rohrbaugh, D. K. *J. Am. Chem. Soc.* **1990**, *112*, 6621–6627.
(9) Wagner, G. W.; Yang, Y. C. *Ind. Eng. Chem. Res.* **2002**, *41*, 1925–1928.
(10) Thatcher, G. R. J.; Kluger, R. *Adv. Phys. Org. Chem.* **1989**, *25*, 99–265.
(11) Westheimer, F. H. *Acc. Chem. Res.* **2002**, *1*, 70–78.
(12) Dantzman, C. L.; Kiessling, L. L. *J. Am. Chem. Soc.* **1996**, *118*, 11715–11719.
(13) Seckute, J.; Menke, J. L.; Emnett, R. J.; Patterson, E. V.; Cramer, C. J. *J. Org. Chem.* **2005**, *70*, 8649–8660.
(14) Daniel, K. A.; Kopff, L. A.; Patterson, E. V. *J. Phys. Org. Chem.* **2008**, *21*, 321–328.
(15) McAnoy, A. M.; Paine, M. R. L.; Blanksby, S. J. *Org. Biomol. Chem.* **2008**, *6*, 2316–2326.
(16) Ramond, T. M.; Blanksby, S. J.; Kato, S.; Bierbaum, V. M.; Davico, G. E.; Schwartz, R. L.; Lineberger, W. C.; Ellison, G. B. *J. Phys. Chem. A* **2002**, *106*, 9641–9647.

SCHEME 2. Proposed Ion−Molecule Reactions of HOO^- with 1

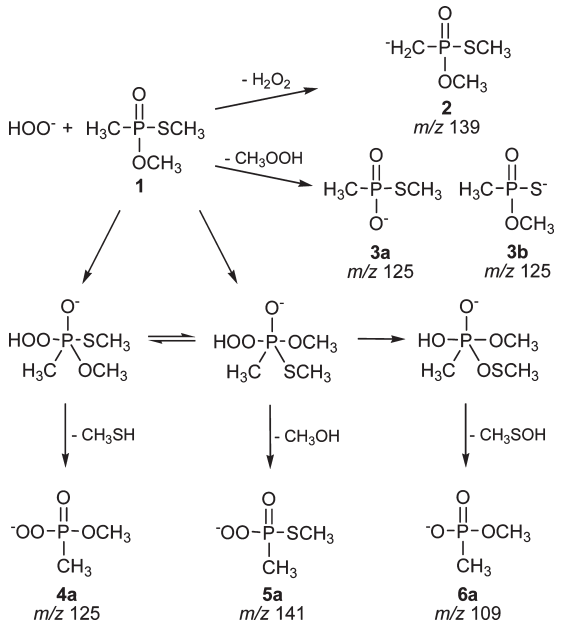

ion pertinent to nerve agent degradation. However, the absence of an addition−elimination pathway in the gas phase reactions of HOO^- with DMMP indicates that this compound, which differs from nerve agents by the absence of P−F or P−S bonds and larger alkyl groups, is not an appropriate model to fully probe nerve agent perhydrolysis. The structure of **1** is similar to that of DMMP except that methylthiolate is substituted for a methoxide and is therefore a more appropriate model compound for VX. Possible product ions which may form during the gas phase reactions of **1** with HOO^- are shown in Scheme 2 and include products of proton transfer (**2**), nucleophilic substitution at carbon (**3a**/**3b**), and nucleophilic addition−elimination at phosphorus involving direct P−S cleavage (**4a**), P−O cleavage (**5a**), or internal sulfur oxidation (**6a**). Significantly, many of these possibilities are distinguishable based on nominal m/z values asserting ion-trap mass spectrometry as an ideal tool to probe these reaction pathways.

Ion−Molecule Reactions of *O*,*S*-Dimethyl Methylphosphonothioate (1). The ion−molecule reactions of **1** with isolated CH_3O^-, $CH_3CH_2O^-$, and HOO^- were conducted with use of a modified linear ion-trap mass spectrometer. The reagent ions were generated in the ion source via negative ion electrospray ionization and **1** was introduced into the ion-trapping region as a gaseous neutral with the helium buffer gas and allowed to react with the isolated reactant ion. The product ions and remaining reagent ions were scanned out of the trap and detected to produce product ion spectra (Figure 1). The alkoxide ions react as gas phase bases and only undergo proton transfer to yield the product ion **2** at m/z 139. The basicities of CH_3O^- ($\Delta_{acid}H_{300}[CH_3OH] = 382.4 \pm 0.5$ kcal mol^{-1}), $CH_3CH_2O^-$ ($\Delta_{acid}H_{300}[CH_3CH_2OH] = 379.1 \pm 0.5$ kcal mol^{-1}),[17] and HOO^- ($\Delta_{acid}H_{300}[HOOH] = 376.5 \pm 0.4$ kcal mol^{-1})[16] are similar and therefore

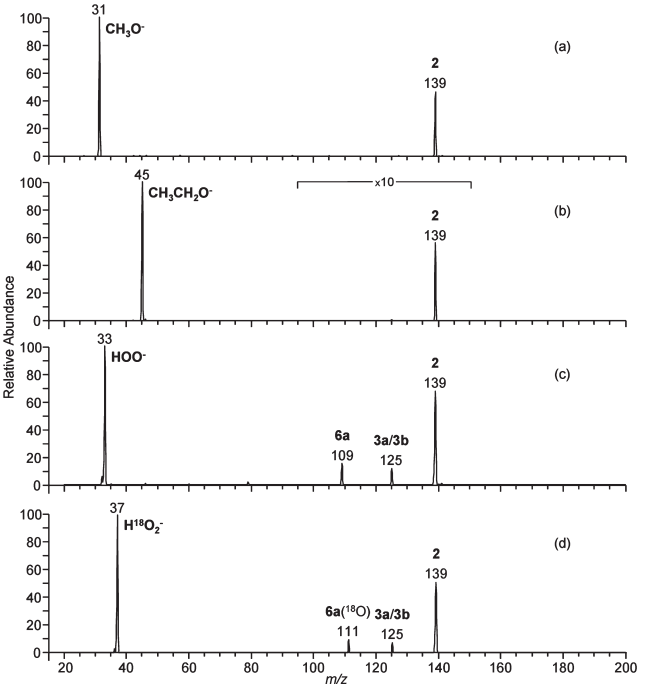

FIGURE 1. Product ion spectra resulting from the gas phase reaction of (a) CH_3O^- (m/z 31), (b) $CH_3CH_2O^-$ (m/z 45), (c) HOO^- (m/z 33), and (d) $H^{18}O_2^-$ (m/z 37) with **1**. In each case, proton transfer yields **2** at m/z 139, while product ions of nucleophilic reactions at m/z 109/111 and 125 are only observed in the reactions of $HOO^-/H^{18}O_2^-$.

reactions of HOO^- with **1** may be expected to only undergo proton transfer. However, the reactions of HOO^- with **1** undergo a proton transfer yielding **2** (m/z 139), with a branching ratio of 74%, and minor nucleophilic processes yielding product ions at m/z 125 and 109 with branching ratios of 11% and 15%, respectively. The branching ratios were determined with use of the Grawbowski method[18] (Supporting Information) and this analysis shows a downward deviation from linearity of the m/z 139 data and upward deviation of the m/z 125 data at high (>80%) reagent ion consumption. This indicates an onset of secondary processes where m/z 139 product ions react with **1** to yield additional m/z 125 product ions. Conversely, the m/z 109 product ion intensity scales linearly with HOO^- consumption indicating that the m/z 109 ion is a primary product of the reaction between HOO^- and **1** under pseudo-first-order conditions.

The product ions observed at m/z 139, 109, and 125, formed by reaction of HOO^- with **1**, were further characterized with MS^n experiments (Figure 2). Collision-induced dissociation (CID) of the m/z 139 product ion yields a fragment ion at m/z 93 (Figure 2a). A nominal loss of 46 Da for this fragmentation process is attributed to neutral loss of thioformaldehyde from **2**, presumably eliminated via a 5-centered rearrangement involving proton transfer from the methylthiolate to the charged center. This assignment is confirmed by CID of the ^{34}S-isotopologue ion at m/z 141 (Supporting Information) that undergoes loss of ^{34}S-thioformaldehyde (48 Da). Interestingly, loss of formaldehyde (30 Da) via a similar rearrangement process involving the

(17) Ramond, T. M.; Davico, G. E.; Schwartz, R. L.; Lineberger, W. C. *J. Chem. Phys.* **2000**, *112*, 1158–1169.

(18) Grabowski, J. J.; Lum, R. C. *J. Am. Chem. Soc.* **1990**, *112*, 607–620.

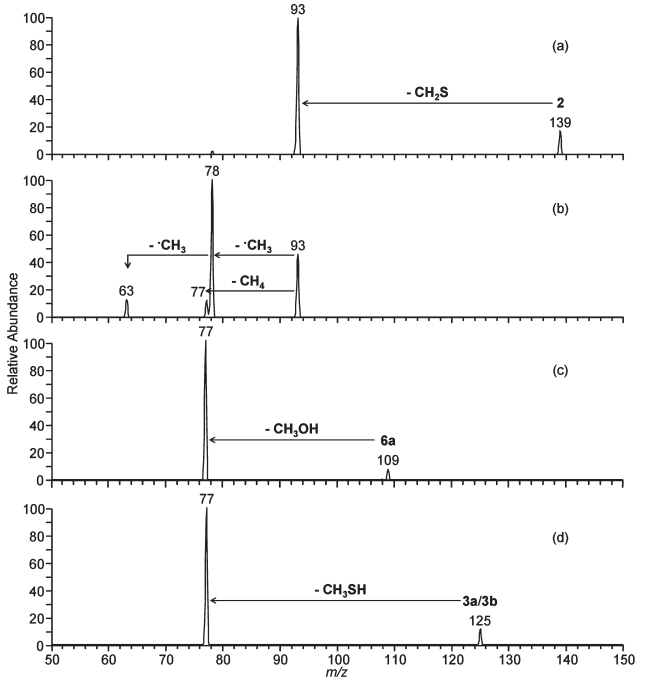

FIGURE 2. MS^n spectra of product ions formed by the reaction of HOO^- with **1**: (a) CID of **2** (MS^3 of m/z 33 → 139), (b) CID of the m/z 93 fragment ion (MS^4 of m/z 33 → 139 → 93), (c) CID of **6a** (MS^3 of m/z 33 → 109), and (d) CID of **3a/b** (MS^3 of m/z 33 → 125).

methoxide is not observed indicating the cleavage of the P−S bond to lose thioformaldehyde is significantly favored over cleavage of the P−O to lose formaldehyde. The CID spectrum of the resulting m/z 93 fragment ion (Figure 2b) shows a major fragment ion at m/z 78 and minor fragment ions at m/z 77 and 63. These can be attributed to the respective losses of CH_3, CH_4, and 2 × CH_3 (or CH_2O) and are in agreement with previously reported MS^n experiments.[15]

Interestingly, the m/z 109 product ion can be attributed to **6a** formed as a result of the proposed sulfur oxidation mechanism. The pathway for m/z 109 formation was further investigated by comparison of CID data of the m/z 109 product ion with CID data of an authentic **6a** ion and, ultimately, with ^{18}O-isotope labeling experiments that, by tracking oxygen atoms originating from the incipient $H^{18}O_2^-$ ion, allow differentiation of the competing pathways described in Scheme 2. The CID spectrum of the m/z 109 product ion (Figure 2c) shows only one fragment ion at m/z 77 due to neutral loss of methanol (32 Da) and is consistent with a product ion structure of **6a**. An ion of known structure **6a** was generated by negative electrospray ionization of methyl hydrogen methylphosphonate (**9**). The CID data of the m/z 109 product ion are in agreement with the CID data of the authentic **6a** ion produced under similar experimental conditions (Supporting Information) indicating the ions have the same structure. Finally, the ^{18}O-labeled HOO^- ion (m/z 37) was generated by electrospray ionization of an infused 3% solution of $H_2{}^{18}O_2$ and allowed to react with **1** in the ion-trap. A mass shift from m/z 109 to 111 was observed in the resulting product ion spectrum (Figure 1d) indicating incorporation of an ^{18}O atom into the product ion. These data unequivocally identify the m/z 109 product ion as **6a** and provide the first experimental evidence of intramolecular sulfur oxidation occurring in this VX model system.

The observed product ion intensity at m/z 125 is consistent with the formation of three distinct product ions from two reaction processes, namely S_N2 at carbon forming product ions **3a**/**3b** and addition−elimination with P−S cleavage forming product ion **4a**. The CID of the m/z 125 product ion results in the exclusive formation of a fragment ion at m/z 77 (Figure 2d) and can be attributed to the neutral loss of thiomethanol (48 Da) from **3a**/**3b**. This assignment was confirmed by CID of the ^{34}S-isotopologue ion at m/z 127 (Supporting Information) that undergoes loss of ^{34}S-thiomethanol (50 Da). Interestingly, the m/z 125 product ion(s) do not undergo loss of methanol suggesting that the decomposing ion is **3a**. This may be explained in terms of the initial S_N2 reaction of HOO^- favoring attack at the methoxide over the thiolate and/or facile rearrangement from **3b** to **3a** upon collisional activation immediately prior to decomposition. The addition−elimination product ion **4a** could conceivably undergo neutral loss of CH_3OOH (48 Da) upon collisional activation and therefore may also contribute to the m/z 125 product ion. However, **4a** may be expected to undergo some loss of methanol, which is not observed. Further, ^{18}O-labeling would result in a mass shift of **4a**, from m/z 125 to 129, due to the incorporation of two ^{18}O atoms. No mass shift is observed during the ^{18}O-labeled experiments consistent with the m/z 125 product ion being formed by an S_N2(carbon) process, indicating that the addition−elimination with P−S cleavage does not occur in this system.

The addition−elimination pathway resulting in P−O cleavage would be expected to yield product ion **5a** at m/z 141. However, CID of the m/z 141 ion is consistent with the ^{34}S-isotopologue of **2** (as discussed above) and no significant ion intensity is observed at m/z 143 for the ^{34}S-isotopologue of **5a**. Further, incorporation of two ^{18}O atoms during the ^{18}O-labeled experiments would mass shift the P−O cleavage product ion by 4 Da. Therefore, the absence of an m/z 145 product ion in the reactions of $H^{18}O_2^-$ with **1** (Figure 1d) indicates that the P−O cleavage pathway does not occur in this system.

Calculated Reaction Pathways. Gas phase proton transfer reactions are thermodynamically controlled and the intensity of facile proton transfer from **1** to HOO^- indicates **1** has a significantly lower enthalpy of deprotonation relative to hydrogen peroxide ($\Delta_{acid}H_{300}$[HOOH] = 376.5 ± 0.4 kcal mol^{-1}).[16] The acidity of **1** has not been reported, but comparison of zero point energy corrected electronic energies of **1** and **2**, at the B3LYP/aug-cc-pVTZ//B3LYP/6-31+G(d) level of theory, estimates this to be 364.8 kcal mol^{-1} (Table 1). On the basis of calculations at the same level of theory,[15] the acidity of DMMP is calculated to be 371.9 kcal mol^{-1} and is in close agreement with the experimental value of $\Delta_{acid}H_{300}[CH_3PO(OCH_3)_2]$ = 373 ± 3 kcal mol^{-1}.[19] The low acidity value of **1** compared to that of hydrogen peroxide explains the dominance of **2** in the product ion spectrum. The pathways of the nucleophilic reactions between HOO^- and **1** (Scheme 2) were similarly investigated at the same level of theory to explain the observation, or absence, of ions in the product ion spectrum.

(19) Lum, R. C.; Grabowski, J. J. *J. Am. Chem. Soc.* **1993**, *115*, 7823–7832.

TABLE 1. Calculated Data for Reactions of 1 with HOO^- Approaching Opposite SCH_3

	electronic energy[a]	zero point correction[a]	relative energy[b]
1	−1009.853082	0.125293	
2	−1009.271696	0.110303	364.8
HOO^-	−150.997306	0.012921	
1 + HOO^-			22.2
a1	−1160.885788	0.139191	0.0
TS 1−3a	−1160.868994	0.139060	10.5
3a	−970.049369	0.084721	
CH_3OOH	−190.884064	0.054687	
3a + CH_3OOH			−29.9
TSa1a2	−1160.880684	0.140438	3.2
a2	−1160.903059	0.142195	−10.8
TSa2a3	−1160.901010	0.141799	−9.6
a3	−1160.905426	0.141968	−12.3
TSa3a4	−1160.906140	0.141682	−12.8
a4	−1160.917754	0.140528	−20.1
4a	−722.191900	0.090517	
4b	−722.175495	0.089062	
CH_3SH	−438.710632	0.046301	
4a + CH_3SH			−10.5
4b + CH_3SH			−0.2
7	−722.749535	0.103788	
CH_3S^-	−438.144250	0.036149	
7 + CH_3S^-			−5.0

[a]Energies (hartrees) calculated at the B3LYP/aug-cc-pVTZ//B3LYP/6-31+G(d) level of theory and include zero point correction. [b]Relative energies (kcal mol^{-1}) are relative to **a1**, except for that of **2**, which is relative to **1**.

The initial pathways investigated involved the approach of HOO^- toward the phosphorus center directly opposite SCH_3, as would be expected for an addition−elimination process resulting in cleavage of the P−S bond. Relevant energies for the stationary points identified from this starting point are provided in Table 1 and the structures of pertinent stationary points are shown in Figure 3. The reactant ion-neutral complex **a1** is stabilized with respect to the separated reactants by 22.2 kcal mol^{-1}, providing significant complexation energy for further reaction. The approach opposite CH_3S may undergo S_N2(carbon) at methoxide through a calculated barrier of 10.5 kcal mol^{-1} (relative to **a1**) to separated products **3a** and CH_3OOH that are stabilized by an additional 29.9 kcal mol^{-1}. Overall, this simple S_N2-(carbon) process is significantly exothermic (52.1 kcal mol^{-1}) and, combined with a negative activation barrier relative to separated reagents, explains the observation of the m/z 125 product ion.

Nucleophilic addition at phosphorus from **a1** is calculated to have a barrier of 3.2 kcal mol^{-1} and results in a lower energy pentavalent intermediate (**a2**) with HOO^- and SCH_3 groups in the apical positions. The rotation of the equatorial methoxide from the initially formed pentavalent intermediate has a barrier of only 1.2 kcal mol^{-1} and coincides with a significant 0.2 Å increase in the P−S bond. The resulting intermediate (**a3**) has a negative barrier of 0.5 kcal mol^{-1} to P−S bond cleavage and continued methoxide rotation to form **a4**. At the B3LYP/6-31+G(d) level used to optimize the structures the barrier is 0.04 kcal mol^{-1} indicating this is an effectively barrierless process. The resulting ion-neutral complex **a4** is 42.3 kcal mol^{-1} lower than the entrance channel and has sufficient internal energy for proton transfer and subsequent elimination of thiomethanol to yield the product ion at m/z 125. Direct dissociation of the ion-neutral

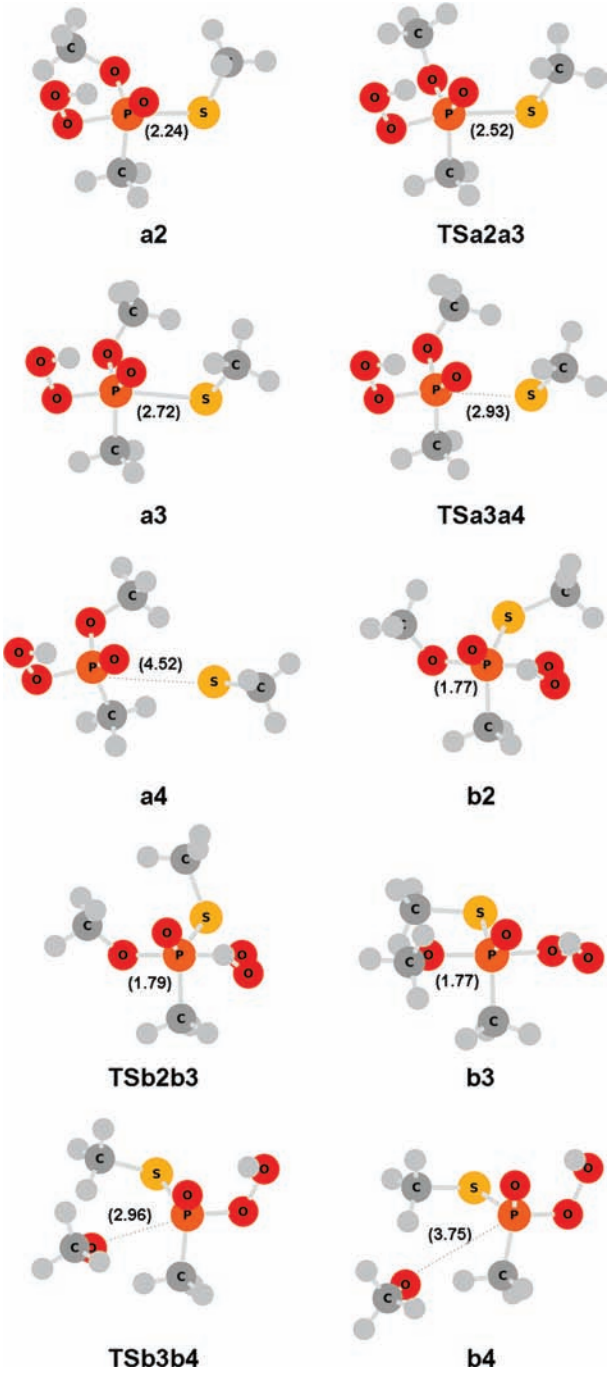

FIGURE 3. Optimized B3LYP/6-31+G(d) geometries of pertinent stationary points on addition−elimination pathways resulting in (a) P−S cleavage and (b) P−O cleavage. P−S or P−O bond distances (Å) are indicated in parentheses.

complex to **7** and CH_3S^- requires 15.1 kcal mol^{-1} while proton transfer and dissociation to the more stable product ion **4b** and CH_3SH requires 9.6 kcal mol^{-1}. However, ^{18}O-labeling data show that **4b** does not contribute to the product ion observed at m/z 125 suggesting there are lower energy and/or more accessible pathways that are more competitive than the P−S cleavage pathway.

Alternative pathways that involved the approach of HOO^- opposite OCH_3 were similarly investigated with relevant energies and structures of stationary points from this

TABLE 2. Calculated Data for Reactions of 1 with HOO^- Approaching Opposite OCH_3

	electronic energy[a]	zero point correction[a]	relative energy[b]
b1	−1160.885597	0.140116	0.1
TS 1−3b	−1160.872354	0.138571	8.4
3b	−970.042277	0.086229	
3b + CH_3OOH			−25.4
TSb1b2	−1160.883926	0.140570	1.2
b2	−1160.904214	0.142108	−11.6
TSb2b3	−1160.889465	0.141995	−3.3
b3	−1160.900006	0.142010	−8.9
TSb3b4	−1160.891066	0.141335	6.7
b4	−1160.881234	0.137350	2.9
5a	−1045.163022	0.087037	
5b	−1045.150267	0.085758	
CH_3OH	−115.725354	0.051291	
5a + CH_3OH			−1.6
5b + CH_3OH			6.4
8	−1045.717062	0.100217	
CH_3O^-	−115.123162	0.035142	
8 + CH_3O^-			28.6
TSb2a3	−1160.889465	0.141995	−2.3
TSb2c3	−1160.893549	0.140661	−4.9
c3	−1160.970755	0.141038	−53.3
TSc3c4	−1160.960086	0.142138	−46.6
c4	−1160.982849	0.141783	−60.9
TSc4c5	−1160.978654	0.141235	−58.3
c5	−1160.981246	0.141787	−59.9
TSc5c6	−1160.982483	0.141079	−60.7
c6	−1160.997888	0.140441	−70.3
6a	−647.071877	0.087779	
6b	−647.012598	0.084979	
CH_3SOH	−513.939344	0.052025	
6a + CH_3SOH			−78.7
6b + CH_3SOH			−41.5
9	−647.604383	0.099950	
CH_3SO^-	−513.368510	0.039039	
9 + CH_3SO^-			−54.7

[a]Energies (hartrees) calculated at the B3LYP/aug-cc-pVTZ//B3LYP/6-31+G(d) level of theory and include zero point correction. [b]Relative energies (kcal mol^{-1}) are relative to **a1**.

starting point provided in Table 2 and Figure 3. The reactant ion-neutral complex **b1** is stabilized with respect to the separated reactants by 22.1 kcal mol^{-1}. As HOO^- approaches **1** opposite the OCH_3 it can also react at the methylthiolate moiety via an S_N2(carbon) process with a barrier of 8.3 kcal mol^{-1} from **b1** to **3b** and CH_3OOH. Similar to the S_N2(carbon) at the methoxide group, this simple S_N2(carbon) process is overall significantly exothermic (47.6 kcal mol^{-1}) explaining the observation of the *m*/*z* 125 product ion. Interestingly, **3b** is slightly higher in energy than **3a** consistent with the experimental results suggesting that the decomposing *m*/*z* 125 ion has structure **3a**.

Nucleophilic addition at phosphorus yielding a pentavalent intermediate with HOO^- and OCH_3 groups in the apical positions (**b2**) is calculated to have a barrier of 1.1 kcal mol^{-1}. Similar to the P−S cleavage pathway, rotation of the equatorial group is needed to facilitate elimination of the apical leaving group. However, the barrier for rotation of the CH_3S group through **TSb2b3** is calculated to be 8.3 kcal mol^{-1} and results in a relatively stable, albeit slightly higher in energy, pentavalent intermediate, **b3**, with no significant effect on the P−O bond. The following step in the process involves cleavage of the P−O bond through **TSb3b4** to yield an ion-neutral complex and is calculated to have a barrier of 15.6 kcal mol^{-1}. The resulting complex **b4** is 19.3 kcal mol^{-1} lower than the entrance channel and, if formed, should have sufficient internal energy for proton transfer and elimination of methanol to yield **5a**,**b** (*m*/*z* 141). Direct dissociation of **b4** to **8** and CH_3O^- requires 25.7 kcal mol^{-1} and is not competitive with respect to proton transfer and elimination of methanol to yield **5a** or **5b** that only requires 3.5 kcal mol^{-1} or releases 4.5 kcal mol^{-1}, respectively.

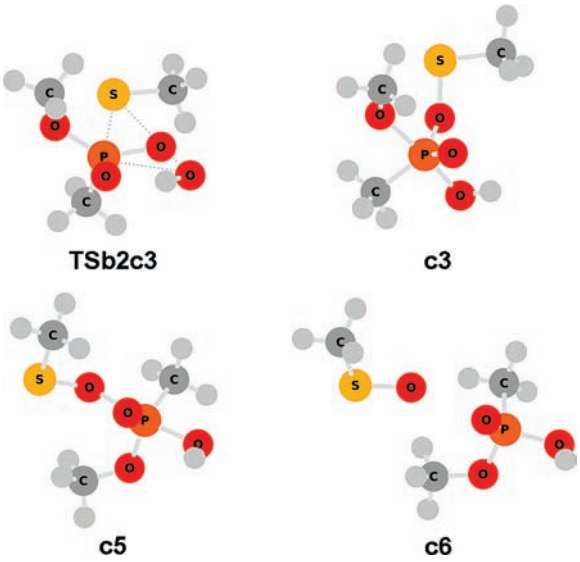

FIGURE 4. Optimized B3LYP/6-31+G(d) geometries of pertinent stationary points for the intramolecular oxygen transfer to sulfur and rearrangement to **c6** that subsequently eliminates CH_3SOH to yield product ion **6a** (*m*/*z* 109).

Interestingly, initial nucleophilic attack opposite the OCH_3 group is considered to be significantly more favored as compared to attack opposite SCH_3, in part, due to the preference for the most electronegative group to occupy the apical position.[10,11] However, no experimental evidence for P−O cleavage has been observed during the perhydrolysis of VX and related compounds indicating an alternate fate of the apparently favored pentavalent intermediate **b1**. It has been proposed that the intermediate leading to P−O cleavage could be a dead end species and always reverts back to reactants.[6] This is consistent with the reverse activation energy for **b3** formation (5.6 kcal mol^{-1}) being significantly lower than the forward barrier for P−O cleavage (15.6 kcal mol^{-1}). However, in the gas phase the initial complexation energy imparted on the system is significantly large that the barrier to P−O cleavage may not fully explain the absence of this pathway. Other pathways proposed for the alternate fate of **b1** involve pseudorotation to an intermediate with apical thiolate and subsequent P−S cleavage or an intramolecular transfer of a hydroperoxy oxygen to the sulfur atom and subsequent elimination of an oxidized sulfur moiety.[7,13] We have calculated a pseudorotation transition state (**TSb2a3**) for conversion of the intermediate **b2** to **a3** that has methylthiolate in the apical position to eliminate thiomethanol as described above (Figure 4). This pseudorotation process has a barrier of 9.3 kcal mol^{-1} and compares to an energy requirement of 18.3 kcal mol^{-1} to invoke the required CH_3S rotation and subsequent P−O bond cleavage from the same intermediate (Table 2). In addition, intermolecular oxygen transfer to sulfur is calculated to have a barrier of

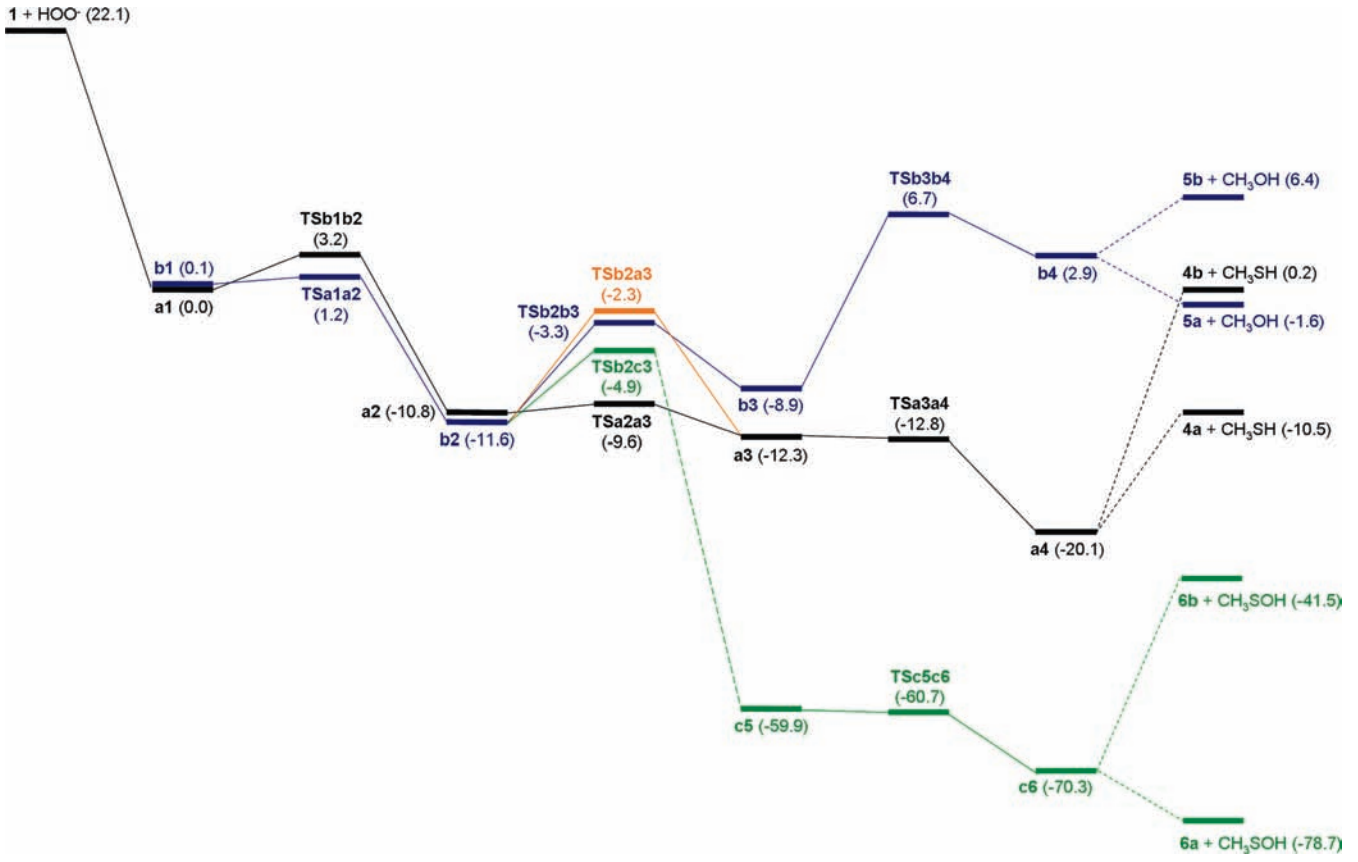

FIGURE 5. Summary of nucleophilic addition pathways for reactions of HOO^- with **1**: addition−elimination with P−S cleavage (**a1** to **a4**), addition−elimination with P−O cleavage (**b1** to **b4**), and sulfur oxidation with elimination of CH_3OSH (**c5** to **c6**, not to scale). Relative energies (kcal mol^{-1}) are calculated at the B3LYP/aug-cc-pVTZ//B3LYP/6-31+G(d) level of theory. (Note: **TSa3a4** and **TSc5c6** are 0.04 and 0.49 kcal mol^{-1} higher than **a3** and **c5** at B3LYP/6-31+G(d), respectively, and indicate small or insignificant barriers for these steps.)

6.7 kcal mol^{-1} and the resulting intermediate **c3** has a reverse activation energy of 48.4 kcal mol^{-1} indicating a major exothermic drive for this reactive pathway (Table 2, Figure 4). Further, the substantial amount of excess energy of **c3** is sufficient for the subsequent rearrangement processes to yield the lower energy ion-neutral complex **c6**. Direct dissociation of **c6** to **9** and CH_3SO^- requires 15.6 kcal mol^{-1} and compares to the elimination of CH_3SOH from **c6** to yield the more stable product ion **6a** that releases an additional 8.4 kcal mol^{-1}. It should also be noted that the above pseudorotation process also provides a channel from the P−S cleavage pathway to intermediate **b2** that can undergo intermolecular oxygen transfer to sulfur. Therefore, all calculated pentavalent intermediates can proceed via the intramolecular sulfur oxidation pathway to CH_3SOH and yield **6a** in a process that is overall exothermic by 100.9 kcal mol^{-1}.

The above calculations explain the observation, abundance, and absence of reaction products of the proposed reaction pathways in the gas phase reactions of HOO^- with **1**. The nucleophilic pathways are summarized in Figure 5, which clearly shows (i) P−O cleavage is not competitive with several lower energy alternative pathways and (ii) internal oxygen transfer is energetically viable and explains the abundance of **6a** in the product ion spectrum. Interestingly, the formation of **b2** is essentially barrierless and would proceed irrespective of the gas phase complexation energy imparted on the system. It follows that **b2** should readily form in solution under ambient conditions and proceed to the exothermic products **4a** and/or **6a**, while the relatively high barrier to P−O cleavage would still prohibit formation of **5a** in solution.

Conclusions

The ion−molecule reactions of HOO^- with **1** have been investigated with a modified linear ion-trap mass spectrometer. The major abundance of **2** in the resulting product ion spectrum is explained by the significantly lower acidity value of **1** relative to that of hydrogen peroxide leading to an extremely efficient proton transfer process. Significant product ions also appearing in the spectrum correspond to the nucleophilic reaction products **3a**/**3b** and **6a**. Simple S_N2 at carbon processes yield **3a**/**3b**, while **6a** is formed as a result of nucleophilic addition at phosphorus affording a reactive pentavalent intermediate that readily undergoes internal sulfur oxidation and concomitant elimination of CH_3SOH. The addition−elimination reaction resulting in cleavage of the P−O bond is not observed in the gas phase and is consistent with its absence in all previous investigations into the alkaline perhydrolysis of VX and related compounds. The elimination of a sulfur moiety deactivates the nerve agent VX and therefore the intramolecular sulfur oxidation process reported here may explain the selective perhydrolysis of the nerve agent to relatively nontoxic products.

Finally, it is of interest that nucleophilic products are not observed in the reactions of CH_3O^- and $CH_3CH_2O^-$ with **1** where only proton transfer is observed. The relative basicities of CH_3O^-, $CH_3CH_2O^-$, and HOO^- are similar and therefore the observation of significant nucleophilic processes in the reactions of HOO^- with **1** may be considered indicative of an enhanced nucleophilicity of HOO^-. We recently detailed dominant nucleophilic processes in the reactions of HOO^- with DMMP, compared to dominant proton transfer for reactions of CH_3O^- with DMMP, as evidence supporting a gas phase α-effect.[15] Meanwhile, an investigation into the S_N2 reactions of α-nucleophiles with alkyl chlorides reported no influence on gas phase reactivity.[20] These experimental studies follow theoretical investigations reporting the existence of gas phase α-effects[21−23] and highlight the complexities of these phenomena are yet to be fully understood.

Experimental Section

Mass Spectrometry. Experiments were performed on a modified linear quadrupole ion-trap mass spectrometer fitted with a conventional electrospray ionization source.[24] Ions were generated by infusion at 3−5 μL min^{-1} of neat CH_3OH, CH_3CH_2OH, or 3% aqueous solutions of H_2O_2, $H_2{}^{18}O_2$ into the electrospray ion source. Typical instrumental settings were as follows: spray voltage −5.0 kV, capillary temperature 200 °C, sheath gas flow between 10 and 30 (arbitrary units), sweep and auxiliary gas flow set at between 0 and 10 (arbitrary units). For collision-induced dissociation (CID) experiments, ions were mass-selected with a window of 1−4 Da, using a Q-parameter of 0.250, and the fragmentation energy applied was typically 10−45 (arbitrary units) with an excitation time of 30 ms. Modifications to the mass spectrometer to allow the introduction of neutral gases into the ion-trap region of the instrument have been previously described.[25] Briefly, neutral liquids and gases are introduced into a flow of Ultra High Purity (UHP) helium (3−5 psi) supplied via a variable leak valve to provide a total ion gauge reading of $\sim 0.9 \times 10^{-5}$ Torr representing an estimated trap pressure of 2.5 mTorr. The temperature of the vacuum manifold surrounding the ion-trap was measured at 307 ± 1 K, which is taken as being the effective temperature for ion−molecule reactions observed herein.[26] For ion−molecule reactions herein, the instrument was operated in low mass mode, the mass cutoff set to m/z 20, and the isolation window varied (8−12 Da) to maximize reagent ion transmission and isolation. Typical reaction times of 10 to 200 ms were set, using the excitation time parameter within the control software using a fragmentation energy of 0 (arbitrary units). All spectra presented represent an average of at least 50 scans.

Synthesis. The phosphonothioate **1** was prepared by a modified procedure and characterization is provided where literature data are absent.[27−29] The phosphonate **9** was prepared according to a literature procedure and had NMR data consistent with those reported previously.[30] Both compounds were obtained to a purity of >95% as determined by ^1H and ^{31}P NMR. EI MS analysis was coupled with gas chromatography and HRMS data were obtained with a FT MS instrument. CAUTION: Organophosphorus compounds can be hazardous and should only be handled in controlled environments.

***O*,*S*-Dimethyl Methylphosphonothioate (1).**[28,29] Oxalyl chloride (2.03 g, 160 mmol) was added in one portion to dimethyl methylphosphonate (2.00 g, 160 mmol) in CH_2Cl_2 (15 mL) and the mixture was refluxed for 8 h. The solvent was evaporated under reduced pressure to yield methyl methylphosphonyl chloride[31] (2.00 g, 97%). A mixture of methyl methylphosphonyl chloride (2.00 g, 160 mmol) in anhydrous THF (15 mL) and sodium methanethiolate (1.12 g, 160 mmol) was stirred for 1.5 h under a nitrogen atmosphere. The mixture was filtered, the solid was washed with CH_2Cl_2, and the solvent was removed from the filtrate under reduced pressure. Flash chromatography (30% acetone/70% hexane on silica) of the residue afforded the *O*,*S*-dimethyl ester, **1**[28,29] (0.560 g, 29%): ^{31}P NMR (202 MHz, DMSO-d_6) δ 56.24 (s); ^1H NMR (500 MHz, DMSO-d_6) δ 1.78 (3H, d, J = 15.5 Hz), 2.23 (3H, d, J = 12.9 Hz), 3.64 (3H, d, J = 12.6 Hz); ^{13}C (126 MHz, DMSO-d_6) δ 12.0 (d, J = 3.5 Hz), 17.8 (d, J = 108.1 Hz), 51.5 (d, J = 7.0 Hz); MS (EI) m/z (rel intensity, %) 140 (70), 125 (14), 110 (13), 93 (100), 79 (37), 63 (31), 47 (24); HRMS (ESI) m/z 141.01334 (MH^+), calcd for $C_3H_{10}PO_2S$ 141.01336.

Electronic Structure Calculations. Geometry optimizations were carried out with the Becke 3LYP (B3LYP) method,[32] using the 6-31+G(d) basis set within Gaussian 03W suite of programs.[33] All stationary points were characterized as either a minima (no imaginary frequencies) or transition states (one imaginary frequency) by calculation of the frequencies, using analytical gradient procedures. Frequency calculations also provided zero point energies, which were used to correct electronic energies calculated with the larger and correlation consistent Dunnings basis set aug-cc-pVTZ.[34] The minima connected by a given transition state were confirmed by inspection of the animated imaginary frequency, using the GaussView package[35] and by intrinsic reaction coordinate (IRC) calculation.[36,37]

Acknowledgment. The authors would like to thank Mr. Alex Theo and Dr. Craig Brinkworth (DSTO) for technical assistance and the Australian Partnership for Advanced

(20) Villano, S. M.; Eyet, N.; Lineberger, W. C.; Bierbaum, V. M. *J. Am. Chem. Soc.* **2009**, *131*, 8227–8233.
(21) Ren, Y.; Yamataka, H. *J. Org. Chem.* **2007**, *72*, 5660–5667.
(22) Ren, Y.; Yamataka, H. *Chem.—Eur. J.* **2007**, *13*, 677–682.
(23) Ren, Y.; Yamataka, H. *Org. Lett.* **2006**, *8*, 119–121.
(24) Schwartz, J. C.; Senko, M. W.; Syka, J. E. P. *J. Am. Chem. Soc. Mass Spectrom.* **2002**, *13*, 659–669.
(25) Harman, D. G.; Blanksby, S. J. *Org. Biomol. Chem.* **2007**, *5*, 3495–3503.
(26) Gronert, S. *J. Am. Chem. Soc. Mass Spectrom.* **1998**, *9*, 845–848.
(27) Hall, C. R.; Inch, T. D.; Pottage, C.; Williams, N. E. *Tetrahedron* **1985**, *41*, 4909–4917.
(28) Hall, C. R.; Inch, T. D. *J. Chem. Soc., Perkin Trans. 1* **1981**, 2368–2373.
(29) Barr, J. D.; Bell, A. J.; Ferrante, F.; La Manna, G.; Mundy, J. L.; Timperley, C. M.; Waters, M. J.; Watts, P. *Int. J. Mass Spectrom.* **2005**, *244*, 29–40.
(30) Kapustin, G. V.; Fejér, G.; Gronlund, J. L.; McCafferty, D. G.; Seto, E.; Etzkorn, F. A. *Org. Lett.* **2003**, *5*, 3053–3056.
(31) Jacobsen, N. E.; Bartlett, P. A. *J. Am. Chem. Soc.* **1983**, *105*, 1613–1619.
(32) Becke, A. D. *J. Chem. Phys.* **1993**, *98*, 1372–1377.
(33) Frisch, M. J.; Burant, J. C.; Millam, J. M.; Iyengar, S. S.; Tomasi, J.; Barone, V.; Mennucci, B.; Cossi, M.; Scalmani, G.; Rega, N.; Petersson, G. A.; Trucks, G. W.; Nakatsuji, H.; Hada, M.; Ehara, M.; Toyota, K.; Fukuda, R.; Hasegawa, J.; Ishida, M.; Nakajima, T.; Honda, Y.; Kitao, O.; Schlegel, H. B.; Nakai, H.; Klene, M.; Li, X.; Knox, J. E.; Hratchian, H. P.; Cross, J. B.; Bakken, V.; Adamo, C.; Jaramillo, J.; Gomperts, R.; Scuseria, G. E.; Stratmann, R. E.; Yazyev, O.; Austin, A. J.; Cammi, R.; Pomelli, C.; Ochterski, J. W.; Ayala, P. Y.; Morokuma, K.; Voth, G. A.; Salvador, P.; Robb, M. A.; Dannenberg, J. J.; Zakrzewski, V. G.; Dapprich, S.; Daniels, A. D.; Strain, M. C.; Farkas, O.; Malick, D. K.; Rabuck, A. D.; Raghavachari, K.; Foresman, J. B.; Cheeseman, J. R.; Ortiz, J. V.; Cui, Q.; Baboul, A. G.; Clifford, S.; Cioslowski, J.; Stefanov, B. B.; Liu, G.; Liashenko, A.; Piskorz, P.; Komaromi, I.; Montgomery, J. A., Jr.; Martin, R. L.; Fox, D. J.; Keith, T.; Al-Laham, M. A.; Peng, C. Y.; Nanayakkara, A.; Challacombe, M.; Gill, P. M. W.; Johnson, B.; Chen, W.; Vreven, T.; Wong, M. W.; Gonzalez, C.; Pople, J. A.; Kudin, K. N. *Gaussian 03*, Revision B.05; Gaussian Inc., Wallingford, CT, **2004**.
(34) Woon, D. E.; Dunning, T. H., Jr. *J. Chem. Phys.* **1993**, *98*, 1358–1371.
(35) Dennington R. K. T., II; Millam, J.; Eppinnett, K.; Hovell, W. L.; Gilliland, R., *GaussView*, Version 4.1; Semichem, Inc., Shawnee Mission, KS, **2003**.
(36) Gonzalez, C.; Bernhard Schlegel, H. *J. Chem. Phys.* **1989**, *90*, 2154–2161.
(37) Gonzalez, C.; Schlegel, H. B. *J. Phys. Chem.* **1990**, *94*, 5523–5527.

Computing for a generous allocation of supercomputing time. A.M.M. acknowledges a DSTO Fellowship Award that supported this project. S.J.B. acknowledges an ARC grant (DP0986738) and thanks UoW and DSTO for their support.

Supporting Information Available: ^{31}P, ^{1}H, and ^{13}C NMR spectra for **1**, ^{31}P and ^{1}H NMR spectra for **9**, CID spectra of ^{34}S-isotopologue ions of **2** and **3a**/**3b**, CID comparison data for authentic **6a** and the *m*/*z* 109 product ion, additional structures of selected stationary points as well as electronic energies, zero point energies, and molecular geometries (as Cartesian coordinates) for all stationary points discussed in the text. This material is available free of charge via the Internet at http://pubs.acs.org.